PHYSICAL REVIEW B VOLUME 46, NUMBER 20 15 NOVEMBER 1992-II

Interfacial reactions and band offsets in the AlSb/GaSb/ZnTe material system

E. T. Yu,* M. C. Phillips, D. H. Chow,† D. A. Collins, M. W. Wang, J. O. McCaldin, and T. C. McGill
T. J. Watson, Sr., Laboratory of Applied Physics, California Institute of Technology, Pasadena, California 91125
(Received 31 July 1991; revised manuscript received 8 June 1992)

We have used x-ray photoelectron spectroscopy to measure valence-band offsets *in situ* for AlSb/ZnTe, AlSb/GaSb, and GaSb/ZnTe(100) heterojunctions grown by molecular-beam epitaxy. For the AlSb/ZnTe heterojunction, a valence-band offset $\Delta E_v = 0.42 \pm 0.07$ eV was obtained. Our data indicated that an intermediate compound, containing Al and Te, was formed at the AlSb/ZnTe(100) interface. Measurements of the AlSb/GaSb and GaSb/ZnTe valence-band offsets demonstrated a clear violation of band offset transitivity for the AlSb/GaSb/ZnTe material system, suggesting that chemical reactivity at the AlSb/ZnTe and GaSb/ZnTe interfaces can exert a significant influence on band offset values. Direct evidence of the influence of interfacial growth conditions on the AlSb/ZnTe and GaSb/ZnTe band offset values was also observed.

I. INTRODUCTION

Recent developments in epitaxial growth techniques for II-VI semiconductors[1–4] have led to considerable interest in the use of these materials in optoelectronic devices; the wide band gaps available in materials such as ZnS, ZnSe, and ZnTe make them particularly attractive for use in visible light emitters. Because of limitations in the dopability of wide-gap II-VI semiconductors, device structures based on the use of heterojunctions to inject carriers into wide-gap II-VI materials have been proposed.[5,6] III-V/II-VI heterojunctions appear to be among the more promising possibilities, but the viability of such approaches depends crucially on band-offset values that for many II-VI and III-V/II-VI heterojunctions are not known.

Another complication that arises for III-V/II-VI heterojunctions is the chemical reactivity of III-V/II-VI interfaces; this tendency has been observed in several previous studies,[7–10] and it is of considerable interest to investigate the possible effect of chemically reacted interface layers on band offsets. Experiments in various material systems have suggested that such effects are possible, with details of interfacial structure appearing to shift band offsets by as much as a few tenths of an electron volt.[11–16] The nearly lattice-matched AlSb/GaSb/ZnTe material system is extremely well suited to studies of these effects—III-V/II-VI interfaces are known to contain intermediate reacted layers, and the existence of three nearly lattice-matched materials allows the transitivity rule to be checked. A clear violation of transitivity would suggest quite strongly that interfacial reactions can exert a sizable influence on band offsets.

In this paper we describe measurements of band offsets and studies of interfacial reactions in the AlSb/GaSb/ZnTe material system. Section II describes the measurement of the AlSb/ZnTe (100) valence-band offset. Comparisons are made with theoretically predicted values for the AlSb/ZnTe valence-band offset, and evidence is presented of chemical reactivity and the formation of an intermediate compound at the AlSb/ZnTe interface. Studies of band-offset transitivity in the AlSb/GaSb/ZnTe material system are presented in Sec. III. The measurement of the AlSb/GaSb band offset is presented in Sec. III A, and the measurement of the GaSb/ZnTe band offset is discussed in Sec. III B. The results of these studies, and in particular the demonstration that transitivity is violated, are discussed in Sec. III C. Attempts to observe the effects of interface reactions on band-offset values more directly are described in Sec. IV. Our conclusions are summarized in Sec. V.

II. AlSb/ZnTe (100)

A. Sample growth

The samples prepared for this study were grown by molecular-beam epitaxy (MBE) in two Perkin-Elmer 430P MBE systems. The AlSb layers were grown in a chamber dedicated to the growth of III-V semiconductors, and the ZnTe layers in a chamber devoted to II-VI semiconductor growth; the two growth chambers and the x-ray photoelectron spectroscopy (XPS) analytical chamber were connected by ultrahigh vacuum (UHV) transfer tubes, allowing samples to be transported among the three chambers without exposure to atmospheric pressure. All samples were grown on *p*-type GaSb (100) substrates, with $p \sim 1 \times 10^{17}$ cm^{-3}. Following oxide desorption at 530 °C, a GaSb buffer layer was grown at 100 Å/min, with the substrate at 475 °C. AlSb layers were grown at 62.5 Å/min with a substrate temperature of 530 °C; for the ZnTe layers, a growth rate of approximately 50 Å/min and substrate temperatures of 270 °C and 330 °C were used.

Al 2*p* core-level to valence-band-edge binding energies were measured in two 5000 Å AlSb layers grown on GaSb buffers. To measure the Al 2*p* to Zn 3*d* core-level energy separation, three samples were grown. Each consisted of over 5000 Å of AlSb grown on a GaSb buffer layer, followed by approximately 25 Å of ZnTe grown at either 270 °C or 330 °C. For the ZnTe layers, streaky reflection high-energy electron diffraction (RHEED) pat-

 ©1992 The American Physical Society

terns were observed within a few seconds after the growths were begun, indicating that growth was two dimensional. For the Zn 3d core-level to valence-band-edge binding energy measurement, an additional 250 Å layer of ZnTe was grown at 270 °C on two of the AlSb/ZnTe heterojunction samples after the heterojunction core-level energy separations had been measured in those samples. The heterojunction samples showed little sign of surface deterioration following the XPS measurements, and streaky ZnTe RHEED patterns were observed almost immediately after growth of ZnTe commenced. Growth of the AlSb/ZnTe heterojunction samples required the use of both MBE chambers, with the samples being transported between the two systems under UHV conditions. Immediately following all growths, the samples were transported under UHV conditions to the XPS chamber for analysis. The ability to perform these experiments without exposing samples to atmosphere allowed us to eliminate experimental uncertainties associated with surface passivation and subsequent evaporation of protective capping layers. This capability was critical in these experiments, given the propensity to form interfacial reaction layers, particularly at the elevated substrate temperatures required for evaporation of surface passivation layers, that seems to be characteristic of III-V/II-VI heterojunctions.

B. XPS measurements and data analysis

Figure 1 shows a schematic energy-band diagram for the AlSb/ZnTe heterojunction. Strain-induced effects on the electronic structure of the two materials have been neglected, due to the small lattice mismatch (0.55%) between AlSb and ZnTe. As shown in the figure, the valence-band offset is given by

$$\Delta E_v = (E_{\text{Al}2p}^{\text{AlSb}} - E_v^{\text{AlSb}}) - (E_{\text{Zn}3d}^{\text{ZnTe}} - E_v^{\text{ZnTe}}) - (E_{\text{Al}2p}^{\text{AlSb}} - E_{\text{Zn}3d}^{\text{ZnTe}}) \ . \quad (1)$$

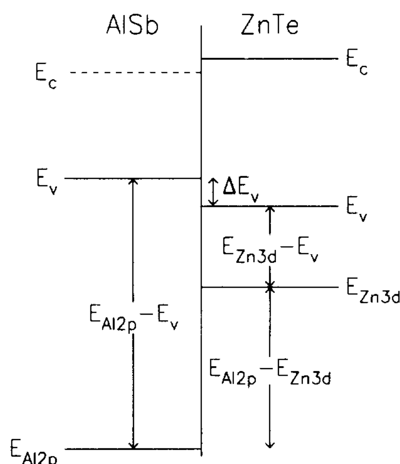

FIG. 1. Schematic energy-band diagram for the AlSb/ZnTe (100) heterojunction. As indicated by the dashed line for the AlSb conduction-band edge, the band gap in AlSb is indirect, with the conduction-band minimum in the Δ direction in the Brillouin zone.

XPS measurements were obtained using a Perkin-Elmer Model 5100 analysis system with a monochromatic Al $K\alpha$ x-ray source ($h\nu = 1486.6$ eV); the pressure in the analysis chamber was typically $\sim 5 \times 10^{-10}$ Torr. For the electron binding energies of interest in our experiments, the typical elastic electron escape depth was approximately 25 Å. Sample XPS spectra for AlSb, ZnTe, and an AlSb/ZnTe heterojunction are shown in Figs. 2(a), 2(b), and 2(c), respectively. The valence-band spectra for the AlSb and ZnTe samples are also shown on enlarged scales, as indicated in the figure.

Core-level peak positions were obtained by subtracting from each core-level peak a background function proportional to the integrated photoelectron intensity and fitting the resulting core-level spectra to characteristic peak-shape functions consisting of two identically shaped Voigt functions separated by a fixed spin-orbit splitting, whose relative heights scaled as $(2J+1)$. The position of a given core level was taken to be an average of the positions of the spin-orbit-split components, weighted by the degeneracy $(2J+1)$. The uncertainty in measured core-level energy separations was estimated to be ± 0.02 eV, and measurements were typically reproducible to ± 0.01 eV.

The position of the valence-band edge in each XPS

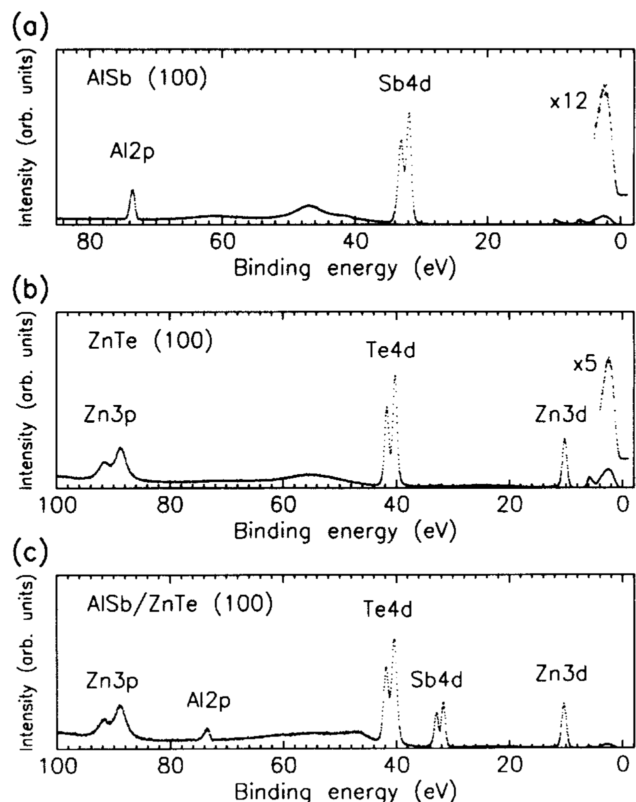

FIG. 2. Representative binding energy XPS spectra for (a) AlSb (100), (b) ZnTe (100), and (c) an AlSb/ZnTe (100) heterojunction. For the AlSb and ZnTe spectra in (a) and (b), respectively, longer sampling times were used in the vicinity of the valence-band edges. The valence-band spectra for the AlSb and ZnTe samples are also shown on enlarged intensity scales, as indicated in the figure.

spectrum was determined using the precision analysis technique of Kraut *et al.*[17] In this approach, the XPS spectrum near the valence-band edge is modeled as a convolution of the valence-band density of states, which we calculate using the empirical pseudopotential method,[18–20] with an experimentally determined XPS instrumental resolution function. This model function is then fitted to the experimental data to give the position of the valence-band edge.

C. Results and discussion

Measurements obtained from the AlSb samples yielded an Al 2*p* core-level to valence-band-edge binding energy of 79.92±0.04 eV. Our measurement is in good agreement with a previously reported value[21] of 72.96 eV. For the ZnTe samples, we obtained a Zn 3*d* core-level to valence-band-edge binding energy of 9.42±0.04 eV. Comparison of this result with previous measurements is difficult, since reported values[22–24] for the Zn 3*d* core-level to valence-band-edge binding energy range from 9.1 to 9.84 eV.

Determination of the Al 2*p* to Zn 3*d* core-level energy separation in the AlSb/ZnTe heterojunctions was complicated by the apparent formation of a reacted layer at the AlSb/ZnTe interface. Evidence of this reaction can be seen in the Al 2*p*, Sb 4*d*, and Te 4*d* core-level spectra from the heterojunction samples. Figure 3 shows Sb 4*d* core-level spectra for AlSb and for an AlSb/ZnTe heterojunction. The AlSb spectrum contains a small component at higher binding energy compared to the main peak; an analogy with observed surface core-level shifts in the As-rich $c(4\times4)$ reconstruction of GaAs[25] suggests that this component may arise from excess Sb on the AlSb surface. The spectrum recorded from a heterojunction sample clearly shows a peak shifted to higher binding energy relative to the main peak structure; this shifted peak was present in all heterojunction samples, independent of the temperature at which the ZnTe layers were grown. By varying the electron takeoff angle from the sample, and therefore the effective electron escape depth, we were able to determine that the smaller, shifted

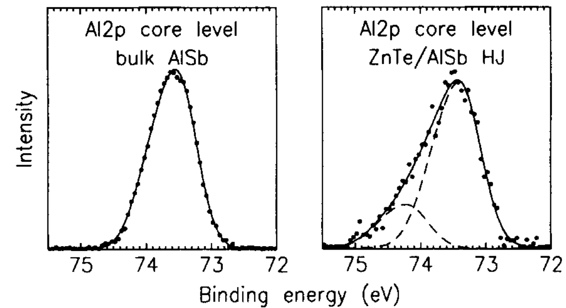

FIG. 4. Al 2*p* core-level XPS spectra from AlSb and from a ZnTe/AlSb heterojunction. The AlSb spectrum contains only a single peak component; the heterojunction spectrum clearly contains a peak shifted to higher binding energy, indicating that Al bonding to Te is present in the reacted layer at the AlSb/ZnTe interface.

peak was due to Sb on the surface of the sample, i.e., on top of the thin ZnTe layer. This conclusion was also supported by the presence of a small but detectable Sb 4*d* core-level peak even for samples with 275 Å of ZnTe deposited on AlSb.

The Al 2*p* core-level spectrum from an AlSb/ZnTe heterojunction, shown in Fig. 4, also exhibits a peak shifted to higher binding energy; the shifted peak is not present in the spectrum in Fig. 4 obtained from pure AlSb. Electronegativity arguments would suggest that Al in the reacted layer is forming bonds with an element more electronegative than Sb, since a shift of the core level to higher binding energy indicates that more charge is transferred away from the Al atom. The only element present that is more electronegative than Sb is Te (2.1 for Te versus 1.9 for Sb on the Pauling electronegativity scale[26]); if Al and Te are indeed forming bonds in the interfacial layer, a peak shifted to lower binding energy should appear in the Te 4*d* spectrum from an AlSb/ZnTe heterojunction. Figure 5 shows Te 4*d* core-level spectra from ZnTe and from an AlSb/ZnTe heterojunction, and a peak shifted to lower binding energy does indeed ap-

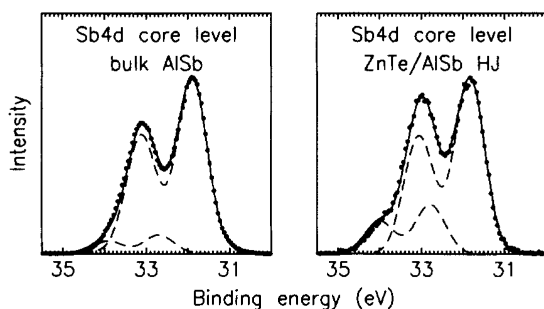

FIG. 3. Sb 4*d* core-level XPS spectra from AlSb and from a ZnTe/AlSb heterojunction. In the AlSb spectrum, the small peak shifted to higher binding energy is thought to arise from excess Sb on the AlSb surface; in the heterojunction spectrum, the peak shifted to higher binding energy was found to originate from Sb at the sample surface, i.e., on top of the ZnTe layer.

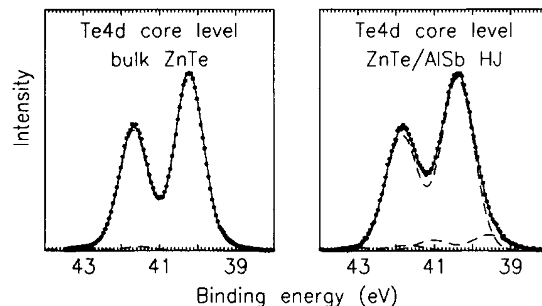

FIG. 5. Te 4*d* core-level XPS spectra from ZnTe and from a ZnTe/AlSb heterojunction. Both spectra contain a small peak shifted to higher binding energy with respect to the main peak; this peak may originate from excess Te at the ZnTe surface. The heterojunction spectrum also contains a peak shifted to lower binding energy, indicating that Te bonding to Al is present in the reacted layer at the AlSb/ZnTe interface.

pear in the heterojunction spectrum. The Te $4d$ spectra also contain very small peaks shifted to higher binding energy; these peaks may be due to excess Te on the ZnTe surface.

The chemical behavior at the AlSb/ZnTe (100) interface thus appears to be quite similar to that observed at a number of other III-V/II-VI heterojunctions. Tu and Kahn[7] observed the formation of an intermediate layer containing Ga and Se at GaAs/ZnSe (110) and (100) interfaces, and detected a layer of Ga_2Se_3 in the wurtzite phase at the GaAs/ZnSe (110) interface. Mackey *et al.*[8] observed evidence that an interfacial layer containing primarily In and Te was formed at InSb/CdTe (100) and (110) interfaces. Wilke *et al.* observed evidence of interfacial reactions and the formation of intermediate compounds composed primarily of the group III and group VI elements in GaSb/ZnTe (110)[9] and CdS/InP (110)[10] heterojunctions. Our measurements and analogies with these other III-V/II-VI heterojunction systems suggest that a compound containing Al and Te is formed at the AlSb/ZnTe (100) interface. An examination of the binary-alloy phase diagram[27] for Al and Te indicates that the most likely candidate is Al_2Te_3.

Taking care to ensure that the measured core-level peak positions were characteristic of pure AlSb and ZnTe rather than of the interfacial layer, we obtained a value of 63.08±0.04 eV for the Al $2p$ to Zn $3d$ heterojunction core-level energy separation; the relatively large uncertainty in this measurement was due to the presence of the chemically shifted component in the Al $2p$ core-level spectrum. Using Eq. (1), we obtain a valence-band offset ΔE_v(AlSb/ZnTe)=0.42±0.07 eV; the corresponding conduction-band offset is $\Delta E_c=0.21\pm0.07$ eV. The band alignment for the AlSb/ZnTe heterojunction is therefore type I, as shown in Fig. 1.

Theoretical predictions for the AlSb/ZnTe valence-band offset encompass a wide range of values. Figure 6 shows the range of values proposed for the AlSb/ZnTe valence-band offset, based on a reported experimental value of 0.40 eV for the AlSb/GaSb valence-band offset[21] and predicted band-offset values for the GaSb/ZnTe heterojunction,[28–39] and also includes the valence-band offset obtained from our measurements. Predictions for the GaSb/ZnTe valence-band offset were combined with the experimental AlSb/GaSb value because of the recognized difficulty of predicting band-offset values directly for heterojunctions with compounds that contain Al.[28–31,33] The serious discrepancies among these theoretical values attest to the need for reliable experimental measurements of band offsets for AlSb/ZnTe and other novel heterojunction systems.

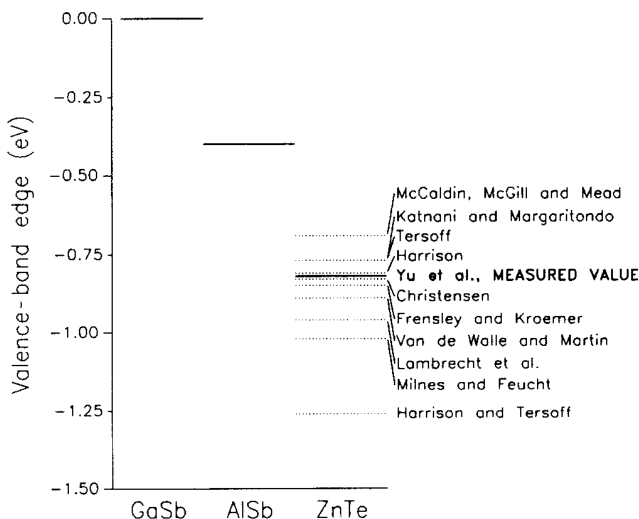

FIG. 6. Proposed valence-band offset values for the AlSb/ZnTe heterojunction, based on a reported experimental value of 0.40 eV for the AlSb/GaSb valence-band offset (Ref. 21) and predicted values for the GaSb/ZnTe valence-band offset; also shown is our measured AlSb/ZnTe valence-band offset, $\Delta E_v=0.42\pm0.07$ eV. Predictions are from the following references: McCaldin, McGill, and Mead (Ref. 28); Katnani and Margaritondo (Refs. 37 and 38); Tersoff (Ref. 32); Harrison (Ref. 30); Christensen (Ref. 39); Frensley and Kroemer (Ref. 31); Van de Walle and Martin (Refs. 34 and 35); Lambrecht, Segall, and Andersen (Ref. 36); Milnes and Feucht (Ref. 29); Harrison and Tersoff (Ref. 33).

III. TRANSITIVITY

To study the effect of the observed interfacial reaction on band offsets, we have checked the validity of the transitivity rule for the AlSb/GaSb/ZnTe material system. The transitivity rule for band offsets is simply the statement that, for three semiconductors A, B, and C, the following relationship should be valid:

$$\Delta E_v(A/B)+\Delta E_v(B/C)+\Delta E_v(C/A)=0 . \quad (2)$$

There exists considerable theoretical and experimental evidence that, for abrupt interfaces, the transitivity rule should be valid. Equation (2) is obviously valid for theories that treat band offsets simply as properties of the bulk constituent materials forming a heterojunction. However, a number of theories that include effects arising from the detailed structure of specific interfaces also yield results that, within the accuracy of the calculations, are consistent with the transitivity rule.[34,36,39–41]

Experimentally, there is substantial evidence that for interfaces of sufficiently high quality, band offsets should obey the transitivity rule. Katnani and Bauer[42] have demonstrated the validity of the transitivity rule for valence-band offsets in the Ge/GaAs/AlAs material system, obtaining band offsets using XPS that satisfy Eq. (2) to within ±0.05 eV. Measurements of Yu, Chow, and McGill[43] and of Hirakawa, Hashimoto, and Ikoma[44] confirming the commutativity of the GaAs/AlAs (100) valence-band offset provide further evidence that band offsets for high-quality, lattice-matched interfaces should be both commutative and transitive. There is also evidence, however, that even in the relatively well-understood Ge/GaAs/AlAs material system, under certain conditions interface chemistry can affect band offset values. Waldrop *et al.*[16] observed that, depending on the interface orientation and surface reconstruction upon which a heterojunction was grown, the GaAs/Ge valence-band offset varied from 0.48 to 0.66 eV. Other measurements by Waldrop *et al.*[45,46] yielded a depen-

dence of the GaAs/AlAs valence-band offset on both interface orientation and growth sequence.

These results indicate that, although the detailed atomic structure of the interface can have a sizable effect on band-offset values, interfaces of sufficiently high quality should exhibit the commutativity and transitivity expected theoretically from abrupt, ideal interfaces. We have therefore attempted to elucidate the influence of interfacial reactions on band-offset values by testing the validity of the transitivity rule for the lattice-matched AlSb/GaSb/ZnTe material system. Measurements were made of the valence-band offsets for the AlSb/GaSb (100) and GaSb/ZnTe (100) heterojunctions, and these values were then combined with our measured AlSb/ZnTe (100) valence-band offset to determine the deviation from the transitivity condition, Eq. (2).

A. AlSb/GaSb (100)

Figure 7 shows a schematic energy-band diagram for the AlSb/GaSb heterojunction. As shown in the figure, the valence-band offset is given by

$$\Delta E_v = (E_{\mathrm{Ga}3d}^{\mathrm{GaSb}} - E_v^{\mathrm{GaSb}}) + (E_{\mathrm{Al}2p}^{\mathrm{AlSb}} - E_{\mathrm{Ga}3d}^{\mathrm{GaSb}}) - (E_{\mathrm{Al}2p}^{\mathrm{AlSb}} - E_v^{\mathrm{AlSb}}) \ . \tag{3}$$

Samples for this study were grown in a Perkin-Elmer 430P MBE system on GaSb (100) substrates, either p type ($p \sim 1\times10^{17}$ cm^{-3}) or degenerately doped n type. Following oxide desorption at 530 °C, a GaSb buffer layer was grown at 100 Å/min, with the substrate at 475 °C. The AlSb layers were grown at 62.5 Å/min with a substrate temperature of 530 °C. All samples were transferred directly from the MBE growth chambers to the XPS analytical chamber under UHV conditions.

The Ga $3d$ and Al $2p$ core-level to valence-band-edge binding energies were measured in GaSb (100) and AlSb (100) films, respectively. The Al $2p$ core-level to valence-band-edge binding energy was measured in two samples, as described in Sec. II. The Ga $3d$ core-level to GaSb valence-band-edge binding energy was measured in one sample, consisting of 5000 Å nominally undoped GaSb grown on a p-type ($p \sim 1\times10^{17}$ cm^{-3}) GaSb (100) substrate. Our measurements yielded a Ga $3d$ core-level to valence-band-edge binding energy of 18.86±0.04 eV, in reasonable agreement with a previously reported value of ~18.90 eV.[21] Figures 8(a) and 8(b) show representative XPS spectra for AlSb (100) and GaSb (100), respectively; the valence-band spectra are also shown on enlarged scales, as indicated in the figure.

The Al $2p$ to Ga $3d$ core-level energy separation was measured in two heterojunctions, one consisting of 25 Å AlSb grown on top of ~5000 Å GaSb, and the other consisting of 20 Å GaSb grown on top of ~5000 Å AlSb. Typical XPS spectra for AlSb grown on GaSb and for GaSb grown on AlSb are shown in Figs. 9(a) and 9(b), respectively. For AlSb grown on GaSb, the separation between the Al $2p$ and Ga $3d$ core levels was measured to be 54.43±0.02 eV; for GaSb grown on AlSb, our measurements yielded an Al $2p$ to Ga $3d$ core-level energy separation of 54.46±0.02 eV. Combining these values, we obtain an Al $2p$ to Ga $3d$ core-level energy separation of 54.45±0.03 eV. Within the range of experimental error, our measurements confirm the commutativity of the valence-band offset for the AlSb/GaSb (100) heterojunction, suggesting that for our AlSb/GaSb interfaces the influence of chemical reactivity is minimal. The slight difference in core-level energy separations for the two

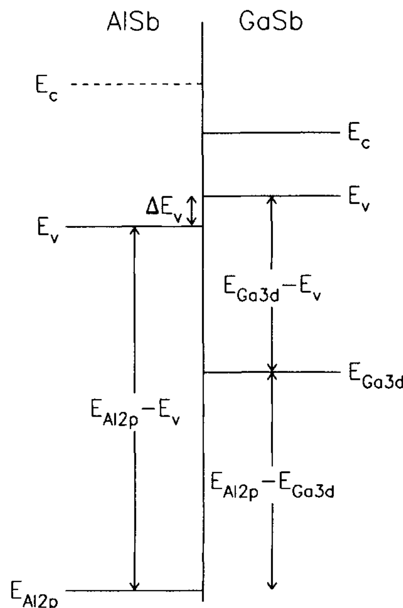

FIG. 7. Schematic energy-band diagram for the AlSb/GaSb (100) heterojunction. As indicated by the dashed line for the AlSb conduction-band edge, the band gap in AlSb is indirect, with the conduction-band minimum in the Δ direction in the Brillouin zone.

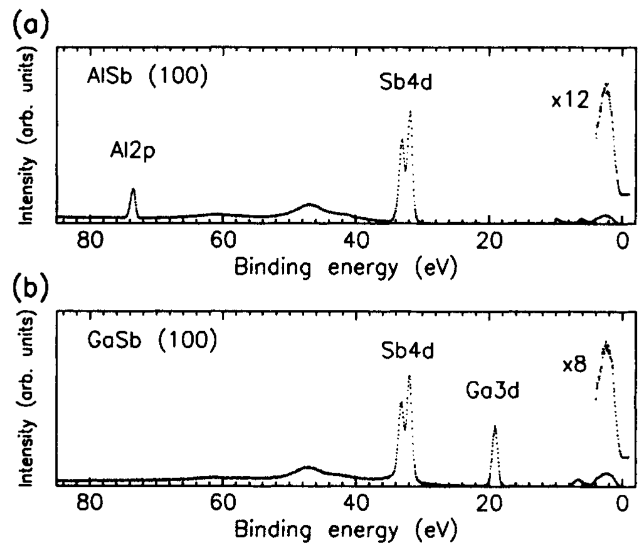

FIG. 8. Representative binding energy XPS spectra for (a) AlSb (100) and (b) GaSb (100). Longer sampling times were used in the vicinity of the valence-band edges to obtain adequate intensities in the valence-band spectra. The valence-band spectra for these materials are also shown on enlarged intensity scales, as indicated in the figure.

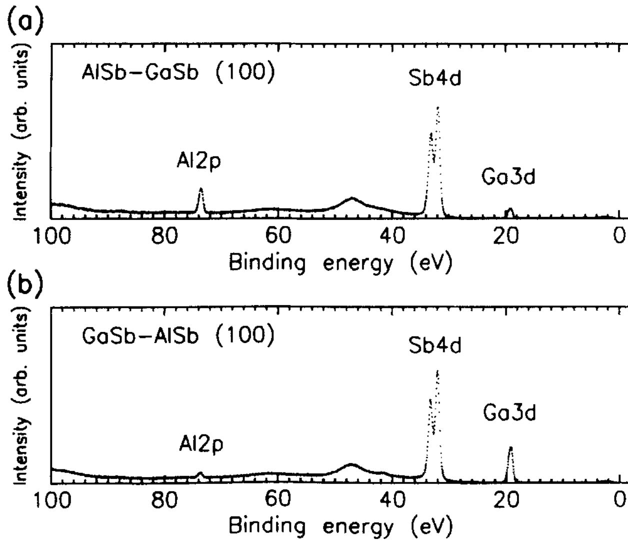

FIG. 9. Representative binding energy XPS spectra for (a) 25 Å AlSb grown on GaSb and (b) 20 Å GaSb grown on AlSb. The Al 2p to Ga 3d core-level energy separation was measured in these samples. Comparing the results from the two different growth sequences allowed the commutativity of the AlSb/GaSb band offset to be checked.

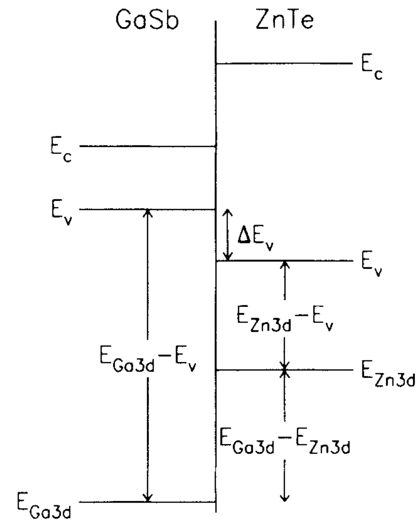

FIG. 10. Schematic energy-band diagram for the GaSb/ZnTe (100) heterojunction. The valence-band offset ΔE_v is obtained by measuring the Ga 3d and Zn 3d core-level to valence-band-edge binding energies in GaSb (100) and ZnTe (100), respectively, and by measuring the Ga 3d to Zn 3d core-level energy separation in a GaSb/ZnTe (100) heterojunction.

different growth sequences could arise from a variety of sources, one notable possibility being the slight lattice mismatch between AlSb and GaSb ($\sim$0.7%). This lattice mismatch should induce strain in the top layer of the heterojunction, resulting in a slight asymmetry for the two growth sequences.

Using Eq. (3), we obtain an AlSb/GaSb valence-band offset $\Delta E_v = 0.39 \pm 0.07$ eV. This measurement is in good agreement with previously reported values. Gualtieri et al.[21] obtained an AlSb/GaSb valence-band offset of 0.40 ± 0.15 eV using XPS measurements, and Menéndez et al.[47] obtained $\Delta E_v(\text{AlSb/GaSb}) = 0.45 \pm 0.08$ eV using a light-scattering method.

B. GaSb/ZnTe (100)

Figure 10 shows a schematic energy-band diagram for the GaSb/ZnTe heterojunction. As shown in the figure, the valence-band offset is given by

$$\Delta E_v = (E_{\text{Ga}3d}^{\text{GaSb}} - E_v^{\text{GaSb}}) - (E_{\text{Zn}3d}^{\text{ZnTe}} - E_v^{\text{ZnTe}}) - (E_{\text{Ga}3d}^{\text{GaSb}} - E_{\text{Zn}3d}^{\text{ZnTe}}) \ . \quad (4)$$

Samples for these measurements were grown on p-type GaSb (100) substrates ($p \sim 1 \times 10^{17}$ cm^{-3}). Following oxide desorption at $\sim$530 °C, a GaSb layer was grown at 100 Å/min, with the substrate at 475 °C. The ZnTe layers were grown at 50 Å/min and using a substrate temperature of 270 °C. The GaSb layers were grown in an MBE chamber dedicated to the growth of III-V semiconductors, and the ZnTe layers in a growth chamber dedicated to II-VI materials. All samples were transferred among the two MBE chambers and the XPS analytical chamber under UHV conditions.

The measurement of the Zn 3d core-level to valence-

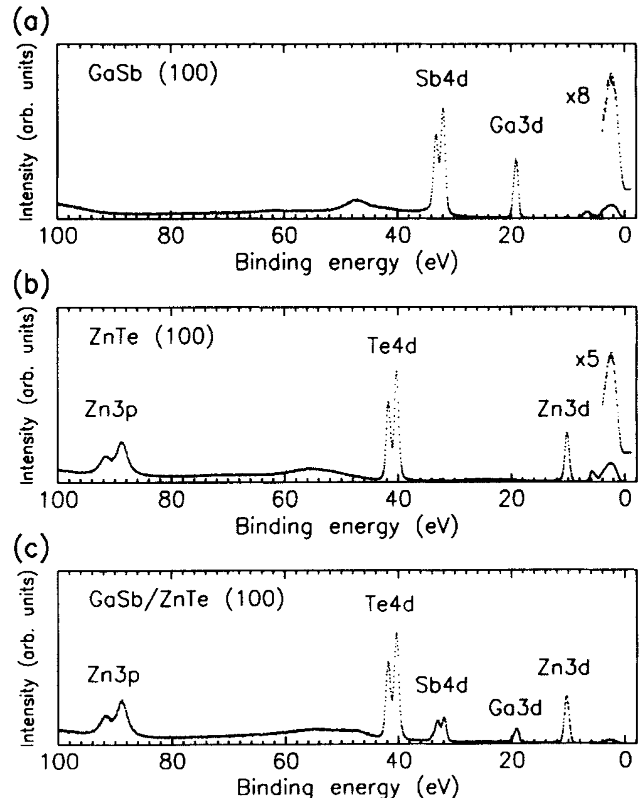

FIG. 11. Representative binding energy XPS spectra for (a) GaSb (100), (b) ZnTe (100), and (c) a GbSb/ZnTe (100) heterojunction. Longer sampling times were used in the vicinity of the valence-band edges to obtain adequate intensity in the valence-band spectra. The valence-band spectra for the GaSb and ZnTe samples are also shown on enlarged intensity scales, as indicated in the figure.

band-edge binding energy in ZnTe was described in Sec. II; the determination of the Ga 3*d* core-level to valence-band-edge binding energy in GaSb was presented in Sec. III A. To measure the Ga 3*d* to Zn 3*d* heterojunction core-level energy separation, a heterojunction sample was grown consisting of ~25 Å ZnTe grown on GaSb. The GaSb surface exhibited an initial (1×3) RHEED pattern; a streaky (2×1) ZnTe RHEED pattern appeared within a few seconds after the ZnTe growths were begun, indicating that growth was two dimensional. Representative XPS spectra for GaSb, ZnTe, and GaSb/ZnTe heterojunctions are shown in Figs. 11(a), 11(b), and 11(c), respectively. The valence-band spectra for the GaSb and ZnTe samples are shown on enlarged scales, as indicated in the figure.

Our measurements yielded a Zn 3*d* core-level to valence-band-edge binding energy of 9.42±0.04 eV, and a Ga 3*d* core-level to valence-band-edge binding energy of 18.86±0.04 eV. Measurements on the GaSb/ZnTe (100) heterojunction sample yielded a Ga 3*d* to Zn 3*d* core-level energy separation of 8.84±0.03 eV. An analysis of Sb 4*d*, Ga 3*d*, and Te 4*d* core-level spectra from GaSb or ZnTe and from the GaSb/ZnTe heterojunction revealed evidence of an interfacial reaction similar to that occurring for the AlSb/ZnTe interface; however, the chemically shifted peaks in core-level spectra from the GaSb/ZnTe heterojunction were less pronounced than those observed in the AlSb/ZnTe heterojunction.

Using Eq. (4), we obtain a GaSb/ZnTe (100) valence-band offset $\Delta E_v(\text{GaSb/ZnTe})=0.60\pm0.07$ eV. This result does not agree well with the value of 0.34±0.05 eV obtained by Wilke and Horn[9] for the GaSb/ZnTe (110) heterojunction. The origin of this discrepancy is unknown, but a number of possibilities exist. Wilke *et al.* observed considerable evidence of a GaSb/ZnTe interfacial reaction, which could affect the value of the band offset differently for their measurement than for ours. In addition, the difference in crystal orientation [(100) for our measurements compared to (110) for Wilke *et al.*] will affect the detailed structure of the interface and could therefore influence the band-offset value. Theoretical values for the GaSb/ZnTe valence-band offset are shown in Fig. 6.

C. Demonstration of nontransitivity

Combining our measured valence-band offsets for the AlSb/ZnTe, AlSb/GaSb, and GaSb/ZnTe heterojunctions of 0.42, 0.39, and 0.60 eV, respectively, we see from Eq. (2) that transitivity for the AlSb/GaSb/ZnTe (100) material system is violated by 0.21±0.05 eV. This discrepancy is far larger than can be accounted for by the experimental uncertainty of our measurements. From Eqs. (1), (3), and (4), one can see that the transitivity rule can be verified simply from the measured core-level energy separations in the three heterojunctions,

$$\Delta E_v(\text{AlSb/ZnTe})+\Delta E_v(\text{AlSb/GaSb})+\Delta E_v(\text{GaSb/ZnTe})=(E_{\text{Ga}3d}^{\text{GaSb}}-E_{\text{Zn}3d}^{\text{ZnTe}})+(E_{\text{Al}2p}^{\text{AlSb}}-E_{\text{Ga}3d}^{\text{GaSb}})-(E_{\text{Al}2p}^{\text{AlSb}}-E_{\text{Zn}3d}^{\text{ZnTe}}) . \tag{5}$$

The uncertainty in determining the deviation from transitivity is therefore determined only by the uncertainty in the measured core-level energy separations, which is much smaller than the total uncertainty in each band offset value. If transitivity were valid for the AlSb/GaSb/ZnTe material system, one would expect Eqs. (2) and (5) to be true to within ±0.05 eV or better; our measurements therefore demonstrate a clear violation of the transitivity rule.

Figure 12 illustrates the deviation from transitivity by placing the conduction- and valence-band edges of AlSb, GaSb, and ZnTe on a common energy scale, with the relative positions of adjacent materials determined by our measured valence-band offsets. As shown in the figure, it is not possible to place all three materials on this common energy scale in a manner consistent with our measurements. This result indicates that, for the AlSb/GaSb/ZnTe material system, band offsets are not determined solely by the properties of the bulk constituent materials, but are strongly influenced by properties of specific interfaces. Our confirmation of commutativity for the AlSb/GaSb (100) valence-band offset suggests that the AlSb/GaSb interfaces are abrupt and that chemical reactivity is relatively unimportant in AlSb/GaSb heterojunctions. Chemical reactions at the AlSb/ZnTe and GaSb/ZnTe interfaces, for which considerable evidence was observed in XPS core-level spectra from AlSb/ZnTe and GaSb/ZnTe heterojunctions, would therefore appear to exert a substantial influence on valence-band offsets in the AlSb/GaSb/ZnTe material system.

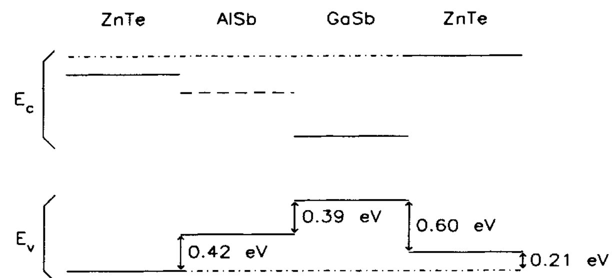

FIG. 12. An illustration of nontransitivity in the AlSb/GaSb/ZnTe material system. The conduction- and valence-band edges of AlSb, GaSb, and ZnTe have been placed on a common energy scale determined by our measured band-offset values; we have measured band offsets between adjacent materials in the figure. It is not possible to place all three materials on a common energy scale consistent with our measurements, indicating that properties of specific interfaces, rather than simply bulk properties, are a major factor in determining band-offset values.

IV. INFLUENCE OF GROWTH CONDITIONS

The observation of nontransitivity of band offsets in the AlSb/GaSb/ZnTe (100) material system, although suggestive, is still only indirect evidence of the influence of III-V/II-VI interface reactions on band-offset values. We have therefore conducted a series of experiments that demonstrate more directly the effect of chemical reactivity on band offset values for the AlSb/ZnTe (100) and GaSb/ZnTe (100) heterojunctions.

Varying the temperature at which the AlSb/ZnTe heterojunction was grown between 270 °C and 330 °C did not have any effect on the value of the AlSb/ZnTe band offset. Petruzzello, Greenberg, and Gaines,[48] however, have reported that the structural quality of ZnSe grown on GaAs is strongly influenced by exposure of the GaAs surface to an initial flux of Zn or Se prior to growth of the ZnSe layer. Initial exposure of the substrate to a Zn flux led to extremely high structural quality at the interface and throughout the ZnSe film, whereas initial exposure to a Se flux resulted in a significant deterioration in sample quality. We have therefore studied the effect on band-offset values in III-V/II-VI heterojunctions of exposing the III-V substrate surface to an initial Zn flux just prior to growth of ZnTe.

Two samples were grown for this study, one consisting of ~25 Å ZnTe grown on GaSb with the GaSb surface exposed to a Zn flux for ~1 min immediately preceding growth of the ZnTe layer, and one consisting of ~25 Å ZnTe grown on AlSb with the AlSb surface exposed to a Zn flux for 60 sec prior to growth of the ZnTe. Both the GaSb and the AlSb surfaces exhibited sharp (1×3) RHEED patterns before and during exposure to the Zn flux, and a streaky (2×1) ZnTe RHEED pattern was observed within a few seconds after growth of ZnTe commenced.

For the GaSb/ZnTe heterojunction grown with an initial exposure of the GaSb surface to Zn preceding growth of the ZnTe layer, our measurements yielded a Ga $3d$ to Zn $3d$ core-level energy separation of 8.89 ± 0.03 eV, compared to 8.84 ± 0.03 eV for the GaSb/ZnTe heterojunction grown without the initial exposure to Zn. This value corresponds to a valence-band offset of 0.55 ± 0.07 eV, compared to our previous value of 0.60 ± 0.07 eV. The initial exposure to Zn at the interface therefore induces a slightly greater deviation from transitivity. However, the evidence for enhancement or suppression of the interfacial reaction was inconclusive. An analysis of the Ga $3d$ core-level spectrum from the GaSb/ZnTe heterojunction grown with the initial Zn exposure yielded a chemically shifted peak component of similar size to that in the sample grown without the initial exposure, the difference between the two being smaller than the uncertainties inherent in the fitting procedure.

For the AlSb/ZnTe heterojunction grown with an initial Zn exposure at the AlSb/ZnTe interface, we obtained an Al $2p$ to Zn $3d$ core-level energy separation of 63.18 ± 0.03 eV, corresponding to a valence-band offset of 0.32 ± 0.07 eV. Our measurements on AlSb/ZnTe heterojunctions grown without an initial Zn exposure yielded an Al $2p$ to Zn $3d$ core-level energy separation of 63.08 ± 0.03 eV, corresponding to a valence-band offset of 0.42 ± 0.07 eV. In this case, the initial Zn exposure leads to a smaller deviation from transitivity. In addition, an analysis of the Al $2p$ core-level spectra from samples grown with and without an initial exposure to Zn suggests that the Zn treatment does indeed partially suppress the interfacial reaction. The relative height of the chemically shifted component compared to the peak from the bulk AlSb layer is somewhat smaller for the sample grown with the initial Zn exposure, suggesting that the Zn treatment has partially suppressed the formation of the interfacial layer.

These results demonstrate that it is possible, under certain growth conditions, to alter the nature or the degree of chemical reactivity at III-V/II-VI interfaces, and that such alterations can exert a substantial influence on band-offset values in these heterojunctions. For the AlSb/ZnTe heterojunction, the initial Zn flux appeared to suppress partially the interfacial reaction between AlSb and ZnTe, and furthermore reduced the deviation from transitivity observed for AlSb/GaSb/ZnTe, as one would expect for a more abrupt interface.

V. CONCLUSIONS

We have presented a series of studies of band offsets and interfacial reactivity in the AlSb/GaSb/ZnTe (100) heterojunction system. For the AlSb/ZnTe heterojunction, our measurements yielded a valence-band offset of 0.42 ± 0.07 eV, corresponding to a conduction-band offset of 0.21 ± 0.07 eV. Our experiments in the AlSb/ZnTe material system also yielded considerable evidence of a chemical reaction occurring at the AlSb/ZnTe interface. An analysis of the Al $2p$, Sb $4d$, and Te $4d$ core-level spectra from AlSb/ZnTe heterojunction samples demonstrated that an intermediate layer containing primarily Al and Te, probably in the form Al_2Te_3, was formed at the AlSb/ZnTe interface. In addition, our measurements on the heterojunction samples and on thicker (275 Å) layers of ZnTe grown on AlSb indicated that a layer of Sb was present on the ZnTe surface, and moved along the growth front as ZnTe was deposited.

An issue of particular interest was the possible effect of the interface layer on the value of the band offset in this material system. To address this issue, we studied band-offset transitivity in the nearly lattice-matched AlSb/GaSb/ZnTe material system. For lattice-matched material systems, there is considerable theoretical and experimental evidence that band offsets should obey the transitivity rule, provided that the actual experimental interfaces have an atomic structure sufficiently close to that of a perfect crystalline interface. We measured valence-band offsets for the AlSb/GaSb and GaSb/ZnTe heterojunction systems, obtaining values of 0.39 ± 0.07 eV and 0.60 ± 0.07 eV, respectively. Combining our measurements for the AlSb/ZnTe, AlSb/GaSb, and GaSb/ZnTe heterojunctions, we determined that the transitivity rule was violated by 0.21 ± 0.05 eV, suggesting that chemical reactions at the III-V/II-VI interfaces were affecting band offset values. We also verified the commutativity of the AlSb/GaSb valence-band offset,

which indicated that the AlSb/GaSb interfaces in our samples were abrupt and relatively unaffected by chemical reactions.

Attempts were also made to observe more directly the effect of III-V/II-VI interface reactions on band-offset values. By exposing the III-V surfaces to a pure Zn flux immediately preceding growth of the ZnTe layer in the heterojunction, we reduced the valence-band offset in the GaSb/ZnTe heterojunction by 0.05 eV to 0.55 ± 0.07 eV, and in the AlSb/ZnTe heterojunction by 0.10 eV to 0.32 ± 0.07 eV. The shift in the GaSb/ZnTe valence-band offset increased slightly the deviation from transitivity, but the shift in the AlSb/ZnTe valence-band offset decreased the violation of transitivity. In addition, an examination of the Al $2p$ core-level spectra from AlSb/ZnTe heterojunctions grown with and without the initial exposure to Zn at the interface suggested that the initial Zn flux produced a partial suppression of the interface reaction between AlSb and ZnTe. In the case of AlSb/ZnTe, therefore, a partial suppression of the interfacial reaction yielded a band-offset value in closer agreement with the transitivity rule that is expected to be valid for ideal interfaces.

ACKNOWLEDGMENTS

Two of us (E.T.Y. and M.C.P.) would like to acknowledge financial support from the AT&T Foundation and the IBM Corporation, respectively. Part of this work was supported by the Office of Naval Research under Grants Nos. N00014-90-J-1742 and N00014-89-J-1141.

*Permanent address: Department of Electrical and Computer Engineering, University of California at San Diego, La Jolla, CA 92093-0407.

†Permanent address: Hughes Research Laboratories, Malibu, CA 90265.

[1] T. Yao, in *The Technology and Physics of Molecular Beam Epitaxy,* edited by E. H. C. Parker (Plenum, New York, 1985), pp. 313–343.

[2] H. Mitsuhashi, I. Mitsuishi, and H. Kukimoto, J. Cryst. Growth **77**, 219 (1986).

[3] M. C. Phillips, Y. Rajakarunanayake, J. O. McCaldin, D. H. Chow, D. A. Collins, and T. C. McGill, Proc. SPIE **1285**, 152 (1990).

[4] J. Qiu, J. M. DePuydt, H. Cheng, and M. A. Haase, Appl. Phys. Lett. **59**, 2992 (1991).

[5] E. T. Yu, Y. Rajakarunanayake, M. C. Phillips, J. O. McCaldin, and T. C. McGill (unpublished).

[6] J. O. McCaldin and T. C. McGill, J. Vac. Sci. Technol. B **6**, 1360 (1988).

[7] D.-W. Tu and A. Kahn, J. Vac. Sci. Technol. A **3**, 922 (1985).

[8] K. J. Mackey, P. M. G. Allen, W. G. Herrenden-Harker, R. H. Williams, C. R. Whitehouse, and G. M. Williams, Appl. Phys. Lett. **49**, 354 (1986).

[9] W. G. Wilke and K. Horn, J. Vac. Sci. Technol. B **6**, 1211 (1988).

[10] W. G. Wilke, R. Seedorf, and K. Horn, J. Vac. Sci. Technol. B **7**, 807 (1989).

[11] S. P. Kowalczyk, E. A. Kraut, J. R. Waldrop, and R. W. Grant, J. Vac. Sci. Technol. **21**, 482 (1982).

[12] F. Xu, M. Vos, J. P. Sullivan, Lj. Atanasoska, S. G. Anderson, J. H. Weaver, and H. Cheng, Phys. Rev. B **38**, 7832 (1988).

[13] D. W. Niles, G. Margaritondo, P. Perfetti, C. Quaresima, and M. Capozi, Appl. Phys. Lett. **47**, 1092 (1985).

[14] D. W. Niles, E. Colavita, G. Margaritondo, P. Perfetti, C. Quaresima, and M. Capozi, J. Vac. Sci. Technol. A **4**, 962 (1986).

[15] P. Perfetti, C. Quaresima, C. Coluzza, C. Fortunato, and G. Margaritondo, Phys. Rev. Lett. **57**, 2065 (1986).

[16] J. R. Waldrop, E. A. Kraut, S. P. Kowalczyk, and R. W. Grant, Surf. Sci. **132**, 513 (1983).

[17] E. A. Kraut, R. W. Grant, J. R. Waldrop, and S. P. Kowalczyk, Phys. Rev. B **28**, 1965 (1983).

[18] M. L. Cohen and T. K. Bergstresser, Phys. Rev. **141**, 789 (1966).

[19] L. R. Saravia and D. Brust, Phys. Rev. **176**, 915 (1968).

[20] J. R. Chelikowsky, D. J. Chadi, and M. L. Cohen, Phys. Rev. B **8**, 2786 (1973).

[21] G. J. Gualtieri, G. P. Schwartz, R. G. Nuzzo, and W. A. Sunder, Appl. Phys. Lett. **49**, 1037 (1986).

[22] G. P. Schwartz, G. J. Gualtieri, R. D. Feldman, R. F. Austin, and R. G. Nuzzo, J. Vac. Sci. Technol. B **8**, 747 (1990).

[23] R. W. Grant, E. A. Kraut, S. P. Kowalczyk, and J. R. Waldrop, J. Vac. Sci. Technol. B **1**, 320 (1983).

[24] T. M. Duc, C. Hsu, and J.-P. Faurie, Phys. Rev. Lett. **58**, 1127 (1987).

[25] P. K. Larsen, J. H. Neave, J. F. Van der Veen, P. J. Dobson, and B. A. Joyce, Phys. Rev. B **27**, 4966 (1983).

[26] S. M. Sze, *Physics of Semiconductor Devices,* 2nd ed. (Wiley, New York, 1981), p. 277.

[27] *Binary Alloy Phase Diagrams,* edited by T. B. Massalski (American Society for Metals, Metals Park, OH, 1986), Vol. 1, p. 172.

[28] J. O. McCaldin, T. C. McGill, and C. A. Mead, Phys. Rev. Lett. **36**, 56 (1976).

[29] A. G. Milnes and D. L. Feucht, *Heterojunctions and Metal-Semiconductor Junctions* (Academic, New York, 1972).

[30] W. A. Harrison, J. Vac. Sci. Technol. **14**, 1016 (1977).

[31] W. R. Frensley and H. Kroemer, J. Vac. Sci. Technol. **13**, 810 (1976).

[32] J. Tersoff, Phys. Rev. Lett. **56**, 2755 (1986).

[33] W. A. Harrison and J. Tersoff, J. Vac. Sci. Technol. B **4**, 1068 (1986).

[34] C. G. Van de Walle and R. M. Martin, Phys. Rev. B **35**, 8154 (1987).

[35] C. G. Van de Walle, Phys. Rev. B **39**, 1871 (1989).

[36] W. R. L. Lambrecht, B. Segall, and O. K. Andersen, Phys. Rev. B **41**, 2813 (1990).

[37] A. D. Katnani and G. Margaritondo, J. Appl. Phys. **5**, 2522 (1983).

[38] A. D. Katnani and G. Margaritondo, Phys. Rev. B **28**, 1944 (1983).

[39] N. E. Christensen, Phys. Rev. B **37**, 4528 (1988).

[40] N. E. Christensen, Phys. Rev. B **38**, 12 687 (1988).

[41] W. R. L. Lambrecht and B. Segall, Phys. Rev. Lett. **61**, 1764 (1988).

[42] A. D. Katnani and R. S. Bauer, Phys. Rev. B **33**, 1106 (1986).

[43] E. T. Yu, D. H. Chow, and T. C. McGill, Phys. Rev. B **38**, 12 764 (1988).

[44]K. Hirakawa, Y. Hashimoto, and T. Ikoma, Appl. Phys. Lett. **57**, 2555 (1990).

[45]J. R. Waldrop, S. P. Kowalczyk, R. W. Grant, E. A. Kraut, and D. L. Miller, J. Vac. Sci. Technol. **19**, 573 (1981).

[46]J. R. Waldrop, R. W. Grant, and E. A. Kraut, J. Vac. Sci. Technol. B **5**, 1209 (1987).

[47]J. Menéndez, A. Pinczuk, D. J. Werder, J. P. Valladares, T. H. Chiu, and W. T. Tsang, Solid State Commun. **61**, 703 (1987).

[48]J. Petruzzello, B. Greenberg, and J. Gaines, Bull. Am. Phys. Soc. **35**, 237 (1990).